Article No. mb981879 J. Mol. Biol. (1998) 280, 463–474

JMB

Domain Motions in Actin

Rebecca Page[1], Uno Lindberg[2] and C. E. Schutt[1]*

[1]*Department of Chemistry Henry H. Hoyt Laboratory Princeton University Princeton, NJ 08544, USA*

[2]*Department of Zoological Cell Biology, Wenner-Grens Institute, Arrhenius Laboratories for Natural Sciences, Stockholm University S-10691 Stockholm, Sweden*

**Corresponding author*

Previous crystallographic investigations have shown that actin can undergo large conformational changes, even when complexed to the same actin binding protein. We have conducted a formal analysis of domain motions in actin, using the four available crystal structures, to classify the mechanism as either hinge or shear and to quantify the magnitude of these changes. We demonstrate that actin consists of two rigid cores, a semi-rigid domain and three conformationally variable extended loops. Confirming predictions about the nature of the domain rotation in actin based on its structural similarity to hexokinase, we show, using an algorithm previously used only to identify protein hinges, that residues at the interface between the two rigid cores undergo a shear between alternative conformations of actin. Rotations of less than 7° in the torsion angles of five residues in the polypeptides that connect the rigid cores enable one actin conformation to be transformed into another. Because these torsion angle changes are small, the interface between the domains is maintained. In addition, we show that actin secondary structure elements, including those outside the rigid cores, are conformationally invariant among the four crystal structures, even when actin is complexed to different actin binding proteins. Finally, we demonstrate that the current F-actin models are inconsistent with the principles of actin conformational change identified here.

Keywords: actin; rigid domain motions; conformational change; hinge and shear; f-actin models

Introduction

Many processes important for the viability of eukaryotic cells depend upon the capacity of actin to be restructured in a controlled manner by polymerization, depolymerization, cross-linking and anchorage. The efficiency of this restructuring depends on the ability of actin binding proteins to recognize, bind and alter specific structures of actin; e.g. monomeric *versus* filamentous actin, or ADP-bound *versus* ATP-bound actin. Changes in the actin monomer structure itself may be important for the mechanisms underlying these recognition events. Biochemical, spectroscopic, and electron microscopic data have demonstrated that the conformation of actin is variable; it is sensitive to the state of the bound nucleotide, to the identity of the cation bound at the high affinity site and to its state of oligomerization (Allen *et al*., 1996; Frieden *et al*., 1980; Frieden & Parane, 1985; Kim *et al*., 1995; Lepault *et al*., 1994; Orlova & Egelman, 1993, 1995; Orlova *et al*., 1995; Strezelecka-Golaszewska, 1993, 1996). In addition, crystallography has shown that two major domains of actin can rotate with respect to one another (Schutt *et al*., 1993; Chik *et al*., 1996). Since the functionally important conformational changes in actin may involve changes similar to those observed crystallographically, a detailed description of the structural differences between the available actin crystal structures will illuminate the mechanism of conformational change in actin, and indicate how similar changes might be involved in the regulation of the microfilament system.

Many large proteins, including actin, consist of multiple domains, distinct structural units which move as independent, rigid bodies connected by flexible structural elements. Rotations of these domains with respect to one another are important in many biological processes, such as enzyme catalysis, ligand binding and oligomerization (Bennett & Steitz, 1980; Harrison *et al*., 1978). Because these events normally occur on the millisecond to micro-

Abbreviations used: rmsd, root-mean-square deviation; pdb, Protein Data Bank; GAPDH, glyceraldehyde-3-phosphate dehydrogenase; ADH, alcohol dehydrogenase.

0022–2836/98/280463–12 $30.00/0

second timescale, they are not usually hindered by high energy barriers. This implies that multiple conformations of a protein, which are related to one another by domain rotations, are accessible under biological ionic and temperature conditions (Brunger *et al*., 1987; Colonna-Cesari *et al*., 1986; Frauenfelder, 1995; Lesk & Chothia, 1984; Wriggers & Schulten, 1997). The atomic mechanism of these low-energy domain rotations can be elucidated by a detailed comparison of two crystal structures of the same protein in different crystalline environments (Bennett & Huber, 1984; Gerstein *et al*., 1994; Sprang *et al*., 1988; Zhang *et al*., 1995). Such studies have demonstrated that most interdomain rotations fall into two categories: hinging or shearing (Gerstein *et al*., 1994). Hinging occurs when the polypeptide chain linking the domains is short and unconstrained by packing, enabling the backbone atoms in this peptide to undergo large changes in conformation with minimal changes in energy. Shearing occurs when the side-chains of the bridging peptide chain are tightly packed. In these cases, the connecting peptide is generally longer, allowing strain energies to be distributed over more bonds. The individual changes in the backbone atoms along the peptide are small because the range of motion available to these residues is limited by constraints imposed by side-chain interactions (for a review, see Gerstein *et al*., 1994).

Actin is the defining member of the actin-fold family (Flaherty *et al*., 1991) which includes hexokinase, a protein which transfers the γ-phosphate from ATP to a molecule of glucose. Crystallographic observations show that the two domains of hexokinase rotate by 12° with respect to one another upon binding glucose (Bennett & Steitz, 1980). Because of their topological similarity, it has been predicted that actin will change conformation by a similar mechanism (Gerstein *et al*., 1994). Four crystal structures of actin have been determined (Table 1): α-actin complexed to DNase I (Kabsch *et al*., 1990); α-actin complexed to gelsolin-S1 (McLaughlin *et al*., 1993), β-actin complexed to profilin in tight state conditions (Schutt *et al*., 1993); and β-actin complexed to profilin in open state conditions (Chik *et al*., 1996). The first three structures of actin are similar in conformation; the major domains of the two α-actin structures are not rotated with respect to one another while those of α-actin and β-actin differ by 5°. The structure of the open state of β-actin (Chik *et al*., 1996), however, is significantly different from those solved previously. The major domains of actin open up with respect to one another by nearly 10°, resulting in a 25% increase in the solvent accessibility of the bound nucleotide (Chik *et al*., 1996). Comparison of this structure with those previously determined will allow the mechanism of conformational change between these structures to be classified as either hinge-like or shear-like.

A formal analysis of the conformational differences between the available actin crystal structures, with an emphasis on the differences between the open and tight states of β-actin, is described here. Techniques developed for comparing alternative conformations of the same protein (Gerstein & Chothia, 1991) were used to identify which regions of the actin monomer function as rigid domains and which undergo conformational change. The mechanism of conformational change, whether hinge or shear, and the magnitude of these changes were then determined. Finally, the conformations of the monomers of the refined actin filament models (Lorenz *et al*., 1993; Tirion *et al*., 1995) were found to be inconsistent with the constraints on actin structural change identified here.

Results

Actin structure

The actin monomer has two domains, originally termed large and small (although they are now known to be nearly identical in size; Figure 1). Each domain can be divided further into two subdomains; the small domain is composed of subdomains 1 and 2, while the large domain comprises subdomains 3 and 4. The large and small domains may have arisen by a gene duplication event, as they are nearly identical in structural connectivity when subdomains 2 and 4 are considered to be extended loops of subdomains 1 and 3, respectively (Kabsch *et al*., 1990). The nucleotide and the high affinity divalent cation binding sites are located at the interface of the large and small domains, near the base of the cleft (Kabsch *et al*., 1990). The bound nucleotide contacts residues from all four subdomains and functions as the

Table 1. Structures and models used in this analysis

Structures	Resolution	Reference	pdb accession numbers
A. *Actin crystal structures*			
α-Actin:DNase I	2.8 Å	Kabsch *et al*. (1990)	*1atn*
α-Actin:Gelsolin-S1	2.5 Å	McLaughlin *et al*. (1993)	Provided by P. J. McLaughlin
β-Actin:Profilin (3.2 M $(NH_4)_2SO_4$)	2.55 Å	Schutt *et al*. (1993)	*1btf*
β-Actin:Profilin (1.8 M KPO_4)	2.65 Å	Chik *et al*. (1996)	*1hlu*
B. *F-actin model structures*			
Lorenz model	N/A	Lorenz *et al*. (1993)	Provided by M. Lorenz
Tirion model	N/A	Tirion *et al*. (1995)	Provided by M. Tirion

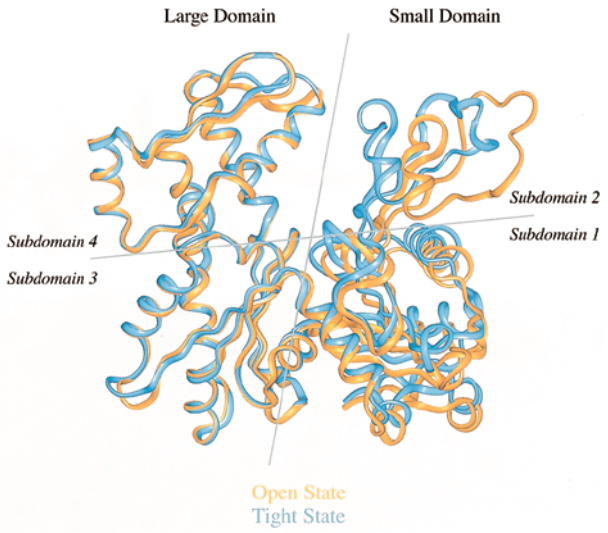

Figure 1. The actin monomer. The domain structure of actin is shown (Kabsch *et al.*, 1990). Actin can be divided into two domains, called large and small, and further divided into subdomains, 1, 2, 3 and 4. The N and C termini are located in subdomain 1. The global difference between the open (gold) and tight (blue) states of β-actin can be described as a rotation of the large domain with respect to the small domain, which results in an opening of the ATP-binding cleft (Chik *et al.*, 1996).

coordinating center of the actin molecule. The global difference between the open and tight states can be described as a rotation of the large domain with respect to the small domain, which results in an opening of the ATP-binding cleft (Chik *et al.*, 1996).

Secondary structural changes

The actin crystal structures were compared to one another not only for changes in domain orientation, but also for changes in secondary and tertiary structure. Changes in local conformation were identified by comparing the secondary structural elements of each actin crystal structure to one another. Specifically, an unbiased, average conformation of each secondary structural element was determined (Gerstein & Altman, 1995). These averaged conformations were then optimally superimposed on their corresponding elements in the actin crystal structures and the rms deviations between them calculated. The average of these rms deviations among the four actin crystal structures represent the conformational variability of each secondary structural element.

Briefly, the unbiased average conformation is determined as follows. A single actin crystal structure is selected and the remaining crystal structures are optimally superimposed onto it. The selected coordinates and the resulting rotated coordinates are then averaged. This is repeated for each actin crystal structure. The averaged coordinates from each set of superpositions are then optimally superimposed on one another. If the averaged coordinates are the same, to within a predefined threshold, then the coordinates constitute the unbiased average conformation of the protein. This process is repeated, with the rotated coordinates representing the new ensemble of structures to be rotated and averaged, until a predefined threshold is reached (Gerstein & Altman, 1995). A threshold of 10^{-3} Å (the accuracy of the coordinates in the pdb files) was used in this study, and was reached, for each secondary structural element, in either two or three iterations of the above procedure.

The only element of secondary structure which had an average rms deviation greater than 0.40 Å was α-helix E205-K215 of subdomain 4, with an average deviation of 0.69 Å between the crystal structures and its average conformation (Figure 2). The α-actin:gelsolin-S1 structure differs most from the others in this region. If this structure is not

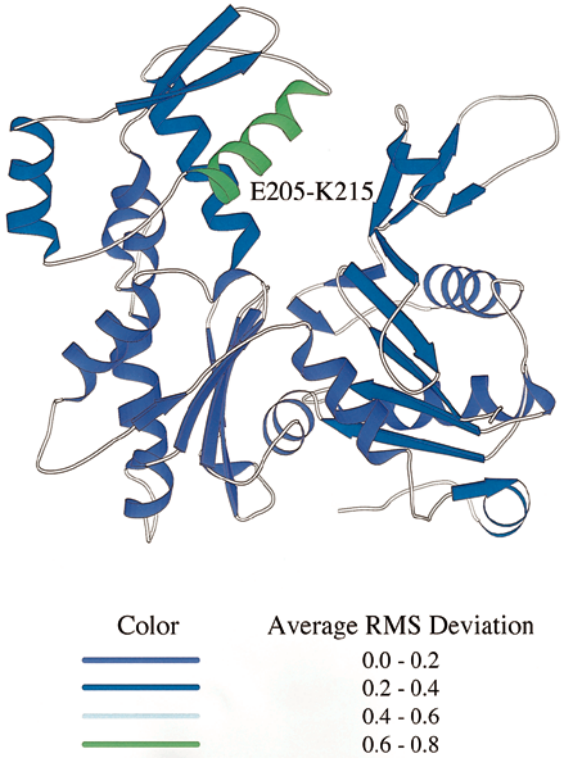

Figure 2. Actin secondary structure is conformationally invariant. An unbiased average conformation for each element of secondary structure in actin was determined (see the text for details) and optimally superimposed on the corresponding elements in each actin crystal structure. The resulting rms deviations from each superposition (four total: α-actin:DNase I and average, α-actin:gelsolin-S1 and average; β-actin: open and average; β-actin:tight and average) were then averaged for each secondary structural element. The average rms deviations of the secondary structural comparisons are mapped onto the β-actin tight state structure using the color scheme shown. As can be observed, most of the secondary structural elements are conformationally invariant, even when actin is complexed to different actin binding proteins.

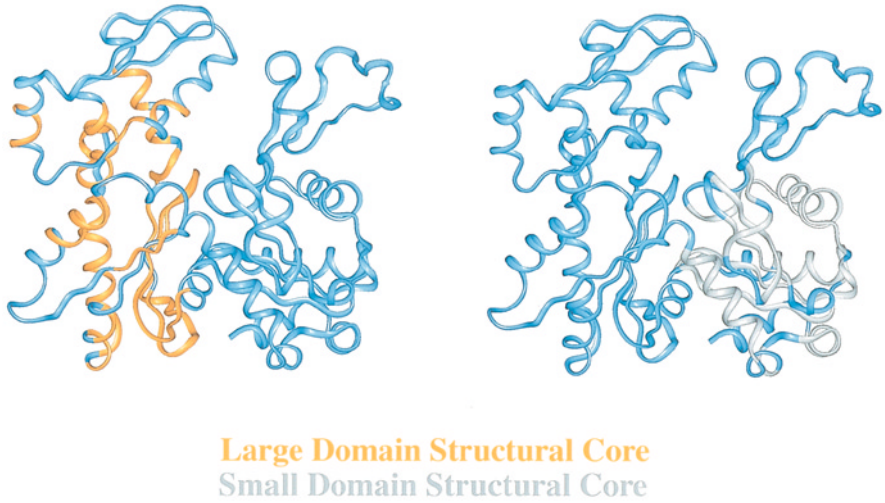

Figure 3. The rigid cores of the actin monomer. Using the *sieve-fit* procedure (see the text for details), the residues which constitute the large domain core (in gold) and the small domain core (in gray) were identified. The large domain core is made up of residues from both subdomains 3 and 4 (see Figure 1), including many residues at the subdomain interface. This shows that most of the large domain functions as a rigid body and, specifically, that subdomains 3 and 4 are not free to rotate independently of one another. The small domain core is composed exclusively of residues from subdomain 1. Contrary to what was observed for the large domain, the small domain core (subdomain 1) and subdomain 2 are free to rotate independently of one another.

included in the average, the rms deviation of this helix drops to 0.37 Å. In all four crystal structures, these residues have high thermal factors, which may contribute to the increased differences in conformation in this region. Thus, even when complexed to different actin binding proteins in crystals, nearly all of the secondary structural elements of the actin monomer are conformationally invariant.

Actin domain structure

The *sieve-fit* algorithm (Lesk, 1991), described below, was used to determine which regions of the actin monomer function as rigid domains. Two sets of coordinates, each set composed of the backbone atoms from a different actin crystal structure, were optimally superimposed on one another. If the calculated rms deviation between the sets was greater than a preset threshold, the distances between corresponding atoms in the sets were calculated. The atoms of the residues furthest apart were then removed from the original sets and the atoms in these reduced sets were superimposed again. This procedure was iterated, with the atoms from a single residue being eliminated in each pass, until the calculated rms deviation dropped below the preset threshold. The residues remaining after the threshold is reached constitute the protein core.

This calculation was carried out for each pairwise combination of the actin crystal structures, using a threshold value of 0.40 Å, the upper bound of the estimated coordinate error of the four structures (Figure 3 and Table 2). As can be observed in Figure 3, the structural core of the actin monomer (henceforth referred to as the large domain core) consists of most of the residues in subdomain 3 and a portion of the residues in subdomain 4. Notably, the core includes the atoms which form the interface between subdomains 3 and 4. This indicates that subdomains 3 and 4 are not conformationally independent of one another, but instead rotate as a rigid unit.

To identify the core of the small domain, the *sieve-fit* procedure was carried out on the small domain alone (residues D2-Q137 and S338-F375; threshold = 0.40 Å). The structural core of the small domain (small domain core) is made up of most of the atoms of subdomain 1, missing only the loops that connect the secondary structural elements to one another. None of the residues of subdomain 2 are included in the small domain core, indicating that it rotates independently of the rest of the small domain. To determine whether subdomain 2 forms an independent core, the *sieve-fit* algorithm was carried out only on residues S33 to H73. Only eight residues remained in the set after the threshold was reached, not enough to constitute a core.

Since the individual secondary structural elements of subdomain 2 were shown to be confor-

Table 2. The residues which constitute the structural cores of actin

Large domain core	145-161, 164-182, 184-185, 188-192, 211-213, 216-217, 225-228, 254-267, 272-286, 288-290, 292-293, 309-315, 330-333
Small domain core	8-12, 16-22, 26-28, 30-31, 74-96, 98-109, 111-112, 118-128, 130-137, 338-349, 354-355, 358-365

See also Figure 3.

mationally invariant between the four crystal structures (Figure 2), it was important to locate the source of the observed conformational difference. The superpositions of these elements among α-actin:DNase I, α-actin:gelsolin-S1 and the β-actin tight state results in rms deviations below 0.40 Å. However, when these elements of the β-actin open and tight states are simultaneously superimposed, the rms deviation is 0.59 Å. This suggests that small shifts between the secondary structural elements take place, characteristic of regions in other proteins that shear (Lesk & Chothia, 1984). Thus, subdomain 2 does not have a true structural core and is better described as a semi-rigid structural unit.

The large domain core, made up of residues from subdomains 3 and 4, and the small domain core, made up of residues from subdomain 1, move as rigid bodies with respect to one another. The large and small domain cores of the β-actin open and tight states each superimpose on one another with an rms deviation of 0.39 Å and 0.38 Å, respectively (Table 3). However, when the two cores are superimposed simultaneously, the rms deviation is 0.99 Å, more than twice the rms deviation for each one alone. This indicates that the domains are rigid and move with respect to one another, and reveals which regions of the actin monomer undergo conformational changes during this transformation. Specifically, these results indicate that the connecting residues, Q137-S145 and P333-S338, are likely candidates for mediating the structural transition between the two states.

Mechanism of conformational change

The *fit-all* algorithm (Gerstein & Chothia, 1991) was used to classify the mechanism of domain rotation as hinge-like or shear-like. In this algorithm, a sequence of the protein suspected of containing a hinge is delineated. All contiguous subsets of this selected polypeptide are then optimally superimposed, and the resulting rms deviations calculated. The superpositions of the subsets which contain residues N-terminal to the hinge will have low rms deviations. As the size of the subset increases to include the putative hinge residue and residues C-terminal to it, the rms deviations will increase significantly if the proteins being compared to one another differ by a rotation at the hinge. If they do not, the rms deviations will remain low. When these rms deviations are displayed in a contour plot (in which the first residue of the superimposed peptide is along the abscissa while the last is along the ordinate) the shape of the contours reveals the presence or absence of a hinge. If the contour lines have a region of high slope and intersect the plot diagonal, the peptide contains a hinge centered on that point. If the contour lines run parallel with the diagonal (which means the rms deviations increase simply because the cumulative error increases with the number of residues being superimposed), the delineated peptide does not contain a hinge residue.

Hinge regions

The *fit-all* procedure was applied to all residues of the open and tight states of β-actin (Figure 4). The hinge and shear regions are denoted by residue numbers along the diagonal of the plot. There are seven regions of high slope in the contour plot, five of which correspond to structural hinges. Residues P38 and D51 delimit the DNase I binding loop in subdomain 2. This loop is extended in the β-actin open state structure and rotates about P38 and D51 to fold back onto subdomain 2 in the tight state structure. The DNase I binding loop, however, does not rotate as a rigid body during this transformation. Many of the residues in this loop differ in conformation from one another between the two states. Specifically, the average difference in the ϕ/ψ angles of residues P38 to D51 are 68.1° and 89.1°, respectively, significantly higher than the average of those in the actin structural cores (Table 4A). In addition, these residues have extremely high *B*-factors (greater than 100 Å^2 in some cases; Table 4B) consistent with the interpret-

Table 3. Superposition of the actin structural cores between the crystal structures and the F-actin models

	Actin crystal structures				F-actin models	
	α-DNase I	α-Gelsolin-S1	β-Tight	β-Open	α-Lorenz[a]	α-Tirion
A. *Large domain core superposition rmsd (Å)*						
α-DNase I	0.00	0.34	0.42	0.41	1.90	1.60
α-Gelsolin-S1		0.00	0.40	0.44	1.99	1.60
β-Tight			0.00	0.38	1.97	1.59
β-Open				0.00	1.99	1.57
α-Lorenz[a]					0.00	2.47
α-Tirion						0.00
B. *Small core superposition rmsd (Å)*						
α-DNase I	0.00	0.32	0.36	0.44	1.75	1.72
α-Gelsolin-S1		0.00	0.35	0.41	1.72	1.71
β-Tight			0.00	0.39	1.74	1.72
β-Open				0.00	1.72	1.72
α-Lorenz[a]					0.00	2.04
α-Tirion						0.00

[a] Residues 262 to 267 and 272 to 274 not included in superposition because they were rebuilt in the Lorenz model.

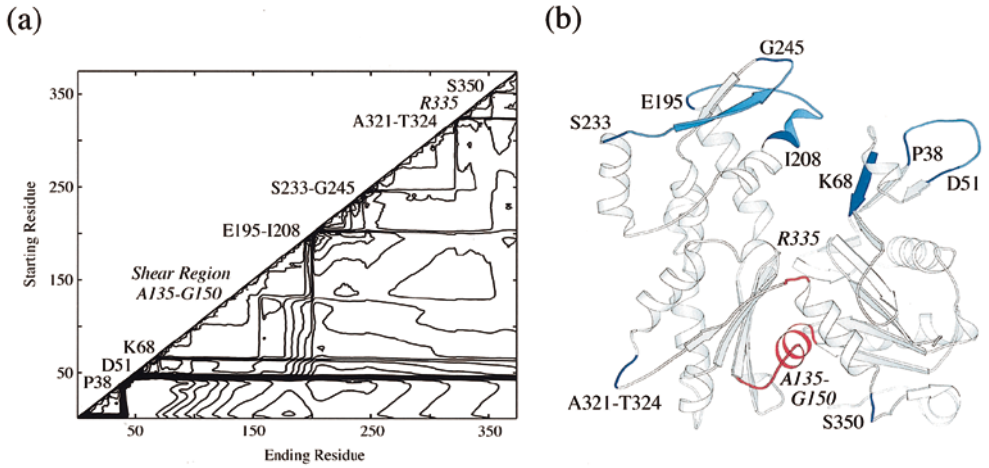

Figure 4. Actin is made up of hinge and shear regions. (a) A contour plot displaying the results of the fit-all procedure (see the text for details) of the β-actin open and tight states. All contiguous polypeptides of the actin monomer (contiguous peptides = 1-2, 1-3, … 1-375, 2-3, 2-4 … 2-375, … 374-375) in both states were optimally superimposed on one another, and the rms deviations between them calculated. The results of the fits are displayed in the above contour plot, in which 30 contours, from 0.0 Å to 4.0 Å are shown. The regions of high slope which intersect the diagonal identify residues which function as hinges. The extended region of high slope which approaches, but never intersects the diagonal, delimits the residues which shear. Six hinge regions (normal font) and two shear regions (italicized font) were identified using the *sieve-fit* algorithm. (b) The positions of the hinge and shear residues are mapped to the β-actin tight state structure. The hinge residues are colored dark blue, the residues in the conformationally variable loops are light blue and the residues in the shear regions are red.

ation that the conformation of this loop is flexible. This loop also differs in conformation between the β-actin tight state and the α-actin:DNase I structures (described by Schutt *et al*., 1993) and is not visible in the electron density maps of the α-actin:gelsolin-S1 structure. Thus, P38 and D51 are not true hinges, in the sense that they are short regions of polypeptide that change conformation between two rigid bodies, but rather function as pseudo-hinges which delimit an entire region of subdomain 2 which is intrinsically flexible.

The next significant difference between the β-actin open and tight states, located near the interface between subdomains 1 and 2, occurs at residue K68. This residue is in the outer strand of the small β-sheet which forms the base of subdomain 2, and both of its backbone atoms are hydrogen-bonded to those of the main-chain atoms of V35 and G36. The global motion of subdomain 2 has been described as a rotation about the central β-strand (V35-R37) of this sheet (Chik *et al*., 1996), which is confirmed by these results. The maintenance of the β-sheet network of hydrogen bonds between strands T66 to K68 and V35 to R37 requires that any changes in the torsion angles of these residues be coordinated. The backbone torsion angle differences beginning at residue T66 and continuing to residue K68 ($\Delta\phi = 19.4°$, $\Delta\psi = 20.7°$) are compensated by similar changes in residues V35 to R37 ($\Delta\phi = 26.0°$, $\Delta\psi = 15.0°$). These torsional changes are higher than the average changes in the residues constituting the actin

Table 4. Average differences in the ϕ/ψ angles and *B*-factors of specified residues

	P38-D51		E195-I208		S233-G245		Structural cores	
	Δφ	Δψ	Δφ	Δψ	Δφ	Δψ	Δφ	Δψ
A. *Average* Δφ/Δψ (°) *between each pair of actin crystal structures*								
α-Gelsolin-S1: β-Tight	N/A[a]	N/A[a]	33.6	57.9	46.6	29.2	11.9	12.5
α-Gelsolin-S1:β-Open	N/A[a]	N/A[a]	70.1	79.4	52.9	49.2	11.1	13.2
α-Gelsolin-S1:α-DNase I	N/A[a]	N/A[a]	30.9	51.9	50.7	45.9	10.7	10.8
α-DNase I:β-Tight	49.2	41.1	26.9	31.4	43.7	48.5	12.7	12.9
α-DNase I:β-Open	74.9	82.1	64.7	48.4	44.8	51.0	12.3	13.0
β-Tight:β-Open	69.0	89.1	53.3	46.5	33.1	45.2	12.1	12.1
Average	64.1	70.8	46.6	52.6	45.3	44.8	11.8	12.4

B. *Average* B-*factors*				
α-Gelsolin-S1	N/A[a]	73.9	73.6	38.1
α-DNase I	15.3[b]	53.1	66.9	32.1
β-Tight	35.0	30.5	29.8	18.4
β-Open	64.4	83.5	31.0	22.8
Average	44.5	55.4	50.3	27.8

[a] This loop is disordered in the Gelsolin-S1 structure.
[b] This loop is bound to DNase I in this structure which may contribute to the low *B*-factors in this region.

cores (Table 4A). In addition, when the small domain cores are superimposed on one another, the distance between the C^{α} atoms of K68 of both structures is only 0.72 Å, but is 2.16 Å between the C^{α} atoms of T66. Yet, the average change in the hydrogen bonding distances of residues T66-K68 to V35-R37 is only 0.06 Å between the two structures, i.e. the β-sheet structure is maintained as it rotates about the central β-strand.

The next two hinges denote structural changes which occur in the regions of E195 to I208 and S233 to G245. These regions are not *bona fide* hinges either, but function similarly to residues P38 and D51 of subdomain 2; i.e. they delimit regions of significant structural change between the open and tight states. Although these changes are not as large as those of the DNase I binding loop, the average ϕ/ψ differences of both structures are still 46.6° and 52.6° for E195 to I208, respectively, and 45.3° and 44.8° for S233 to G245, respectively, compared to 11.8° and 12.4° for the residues in the actin structural cores (Table 4A). Like the residues in the DNase I binding loop, these residues also have high *B*-factors, with an average of 55.4 $Å^2$ and 50.3 $Å^2$, respectively (compared to 27.8 $Å^2$ for the residues in both structural cores; Table 4B). Thus, E195 to I208 and S233 to G245, like P38 to D51, are contiguous regions of the actin monomer which are structurally variable.

Finally, residues A321 and T324 are hinges about which a small loop (A321 to T324) in subdomain 3 rotates as a rigid unit and there is a small increase in slope at residue S350, indicative of a small change in structure near the C terminus of actin (also described by Chik *et al*., 1996).

Shear regions

The most notable feature of the plot in Figure 4 maps to residues A135 and G150. The slopes of the contour lines in this region increase significantly, but the contour lines themselves only approach the diagonal, never intersecting it. This means that the conformational changes in the polypeptide that joins the large and small domain cores are not localized to a single residue, as in hinges, but extend over a number of residues, characteristic of a shear mechanism. To assess the magnitude of these changes, the torsion angles of residues within helix A135 to G150 and loop R335 to S338 were manually adjusted until the large and the small domain cores of the open and tight states could be simultaneously superimposed. This was achieved most simply by rotations in the ϕ angles of residues Q137, A138, L140, L142, and R335 of −1.9°, −2.7°, −6.6°, 1.4° and 4.0°, respectively (Figure 5). After these rotations were applied, the rms deviation between the small domain cores decreased from 1.9 Å to 0.6 Å when the two states had initially been superimposed on the cores of the large domain. It is interesting to note that these rotations are significantly less than the average difference between the ϕ/ψ angles of the core residues. Gerstein *et al*. (1993) have shown that it is often the case that the difference in ψ angles of residues i is approximately equal to the negative difference in ϕ angles of residues $i+1$ of the residues in rigid domains. Of the 190 residues which make up the structural cores in actin, 139 have $\Delta\psi_i \approx -\Delta\phi_{i+1}$ to within 10.0°. Due to this compensation in neighboring torsion angles, the chain direction in the structural cores remains essentially unchanged between the two states. In contrast, the changes in the connecting polypeptide all occur in the ϕ-angles and are not compensated for by corresponding changes in the ψ-angles of the previous residue. This enables these rotations to sum along the helix. Thus, the rotation between the two cores is best described as a shear.

This shear motion is accommodated by small changes in the side-chain torsion angles of the residues which comprise the shear interface. The changes in the χ_1 side-chain torsion angles of the shear interface residues are listed in Table 5. The average difference in the χ_1 angles of these residues between the β-actin open and tight states is 26.5°, indicating that, on average, the side-chains rotate within a single rotamer conformation (i.e. within a single local minimum). One residue, Thr106, changes rotamer conformations, with a $\Delta\chi_1$ of 96.0°. Changes of this magnitude are characteristic of other protein shear interfaces (Gerstein *et al*., 1994).

F-actin models

Two models of the actin filament (F-actin) have been obtained by refining the α-actin:DNase I crystal structure (Lorenz *et al*., 1993; Tirion *et al*., 1995). During refinement, the conformation of the actin crystal structure is changed to optimize its fit with fiber diffraction data. The resultant changes in the α-actin monomer are assumed to reflect conformational changes associated with the polymerization reaction. To determine if the models of F-actin are consistent with the kinds of structural change seen in this analysis, the secondary and tertiary structural elements of the models were compared to those of the unbiased average secondary structure conformations determined previously and the starting crystal structure using methods described above (Figures 6(a) and (b)). In contrast to what was observed for crystallographically distinct actin crystal structures (compare with Figure 2), many elements of secondary structure in both models change significantly during refinement. The largest changes occur in the central β-sheets of subdomains 1 and 3, resulting in rms deviations from 0.8 Å to over 2.0 Å, much higher than those expected for rigid cores. In addition, when both structural cores of the models are optimally superimposed onto those of the initial structure, the rms deviations are over four times that expected on the basis of the coor-

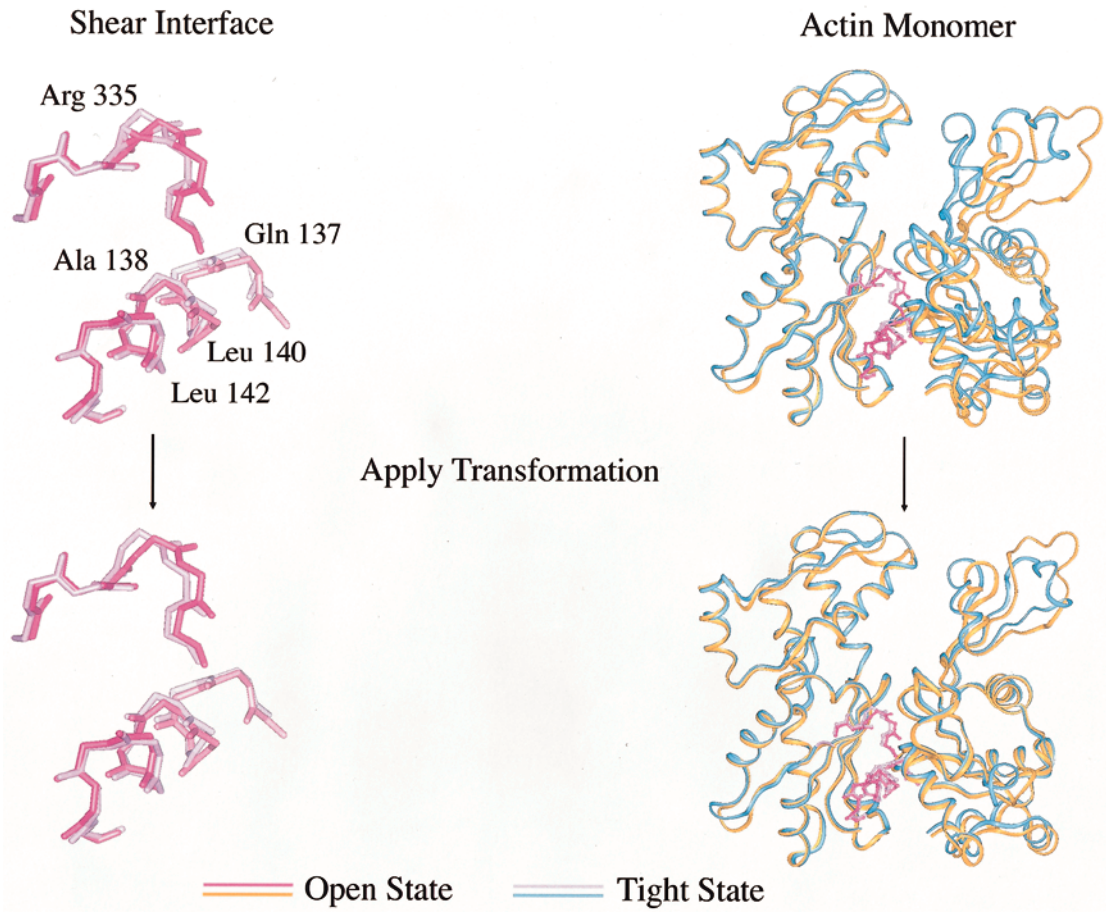

Figure 5. The β-actin open state can be transformed into the tight state by rotations about five torsion angles of the residues which connect the large and small domains. The residues which constitute the shear interface are shown on the left as stick models (dark pink, β-actin, open state; light pink, β-actin, tight state) and the corresponding actin monomers are shown on the right in ribbons (gold, β-actin, open; blue, β-actin, tight). The β-actin open and tight states are superimposed on the large domain core in all four panels. To assess the magnitude of the rotations required to transform the small domain core of the open state onto that of the tight state, the torsion angles of different residues in the shear region, Q137 to S145 and R335 to S338, were changed manually until both the large and small domain structural cores could be superimposed simultaneously on one another. This was achieved by small rotations in the ϕ angles of residues Q137, A138, L140, L142, and R355 by amounts of $-1.9°$, $-2.7°$, $-6.6°$, $1.4°$ and $4.0°$, respectively. The rms deviation between the small domain cores decreases from 1.9 Å to 0.6 Å after these rotations are applied.

dinate errors of the α-actin:DNase I structure (Table 3). One of the more dramatic changes occurs in α-helix W79 to Y91, in which all of the α-helical hydrogen bonds exchange donor:acceptor partners as these residues tighten into a 3_{10}-helix. Thus, if the refined actin filament models are considered to represent the biological actin polymer, the concept that conformational changes in multidomain proteins occur without extensive changes in secondary and tertiary structure within these domains, would not appear to be applicable to the actin polymerization reaction.

Discussion

Actin conformation

This detailed comparison of the four actin crystal structures has revealed several hallmarks of the actin structure. First, actin contains two rigid cores, seven hinge and shear regions, and a semi-rigid domain. The large domain core was defined as those residues which form the largest structurally-invariant domain among all four actin structures. It contains residues from subdomains 3 and 4 (Table 2), including those at the subdomain interface. Thus, subdomains 3 and 4 do not rotate independently of one another, as might have been expected on the basis of the conserved structural connectivity of the large and small domains, but instead rotate as a single, rigid body. Examination of the structure shows that residues F262 to G273 form an outer loop which buttresses both subdomains 3 and 4, and functions to further stabilize the extensive intersubdomain interface. The small domain core, the structurally invariant region of the small domain, only contains residues from subdomain 1. Thus, the small domain core can rotate

Table 5. Relative SASAs[a] and χ_1 angle changes of residues at the shear interface

Residue	Accessible surface area SASA[a] (Å^2)	Relative SASA[b] (%)	χ_1 angle comparisons (°) β-Tight χ_1	β-Open χ_1	$\lvert\Delta\chi_1\rvert$
A. *Shear helix*					
Gln137	26.0	14.4	−56.0	−61.0	5.0
Ala138	0.2	0.2	–	–	–
Val139	22.4	14.5	170.0	−174.0	16.0
Leu140	4.6	2.7	−65.0	−73.0	8.0
Ser141	1.9	1.7	−62.0	−65.0	3.0
Leu142	1.4	0.8	−157.0	−173.0	16.0
Tyr143	84.5	36.7	−152.0	−73.0	*79.0*
Ala144	36.0	31.3	–	–	–
Ser145	34.3	29.8	65.0	64.0	1.0
B. *Additional residues*[c]					
Asp11	7.1	4.7	178.0	−172.0	10.0
Thr106	2.4	1.7	56.0	−135.0	*96.0*
Arg147	62.0	27.6	176.0	−72.0	*76.0*
Val152	0.0	0.0	−176.0	167.0	17.0
Asp154	19.1	12.7	−165.0	−172.0	7.0
Val163	0.0	0.0	178.0	−158.0	24.0
Ile165	0.0	0.0	−69.0	−57.0	12.0
Ser300	0.0	0.0	70.0	40.0	30.0
Ser338	8.1	7.0	−67.0	−117.0	50.0
Val339	15.0	9.7	175.0	176.0	1.0
Ile341	37.7	21.4	−53.0	−93.0	40.0
Ile345	61.9	35.3	−74.0	−51.0	23.0
Leu346	25.9	15.2	−161.0	−144.0	17.0
Average $\Delta\chi_1$					26.5°

[a] Solvent accessible surface Area (SASA) of the residue in the tight state of β-actin.
[b] The amount of solvent accessible surface area of the residue relative to that expected for the same residue free in solution (that is, when the maximum amount of surface is accessible to solvent). The smaller this percentage, the more buried the residue.
[c] Residues which, along with those of the shear helix, form the shear domain interface (all residues are with 5 Å of a residue in the shear helix).

independently of the large domain core, and the semi-rigid subdomain 2 can rotate separately from the small domain core.

Six hinges and a shear region were identified using the *fit-all* algorithm. Three hinge regions actually delimit portions of the molecule which are conformationally variable. These include residues in the extended loops at the top of subdomain 4, E195 to I208 and S233 to G245, and in the DNase I binding loop of subdomain 2, P38 to D51. Comparison of the rms deviations between the secondary structural elements in these regions and of the average differences between the ϕ/ψ angles and the *B*-factors of the backbone atoms of these residues with those of the structural cores (Table 4), confirms that the conformation of all the residues of peptides P38 to D51, E195 to I208 and S233 to G245 differ significantly from one another. These regions are thought to be involved in forming actin:actin contacts in the actin filament (Chik *et al*., 1996; Schutt *et al*., 1995).

Three hinge regions identify residues which function as true hinges. T66 to K68 is a coordinated hinge with residues V35 to P38, about which the semi-rigid subdomain 2 rotates independently of the small domain core. Residues A321 to T324 are also hinges which enable the residues of this small loop to rotate as a rigid body, and, there is a small hinge-like rotation about residue S350, which is indicative of a small change in structure near the C terminus of actin.

Finally, the comparison of the β-actin open state with the other actin crystal structures shows that the majority of the conformational changes observed between the β-actin open and tight states are due to shearing which occurs between the two core domains along two regions of the polypeptide. The 10° relative rotation between these domains results in an opening of the ATP binding cleft, making the ATP ligand over 25% more accessible to solvent (Chik *et al*., 1996). The shearing of the two cores can be most simply simulated by small changes in the ϕ angles of five residues. When the large domain cores of the β-actin open and tight states are superimposed on one another, the rms deviation between the small domain cores is 1.9 Å. After the ϕ angles of residues Q137, A138, L140, L142 and R335 are rotated by −1.9°, −2.7°, −6.6°, 1.4° and 4.0°, respectively, the rms deviation between the small domain cores drops to 0.6 Å. These rotations are small and the residues remain in conformationally allowed regions of Ramachandran space during this transition. The shear transition is accommodated by small rotations, an average of 26.5°, of the χ_1 torsion angles of the side-chains of the residues which comprise the interface (Table 5).

Shear mechanism

Actin was predicted to change conformation *via* a shearing mechanism based on its structural simi-

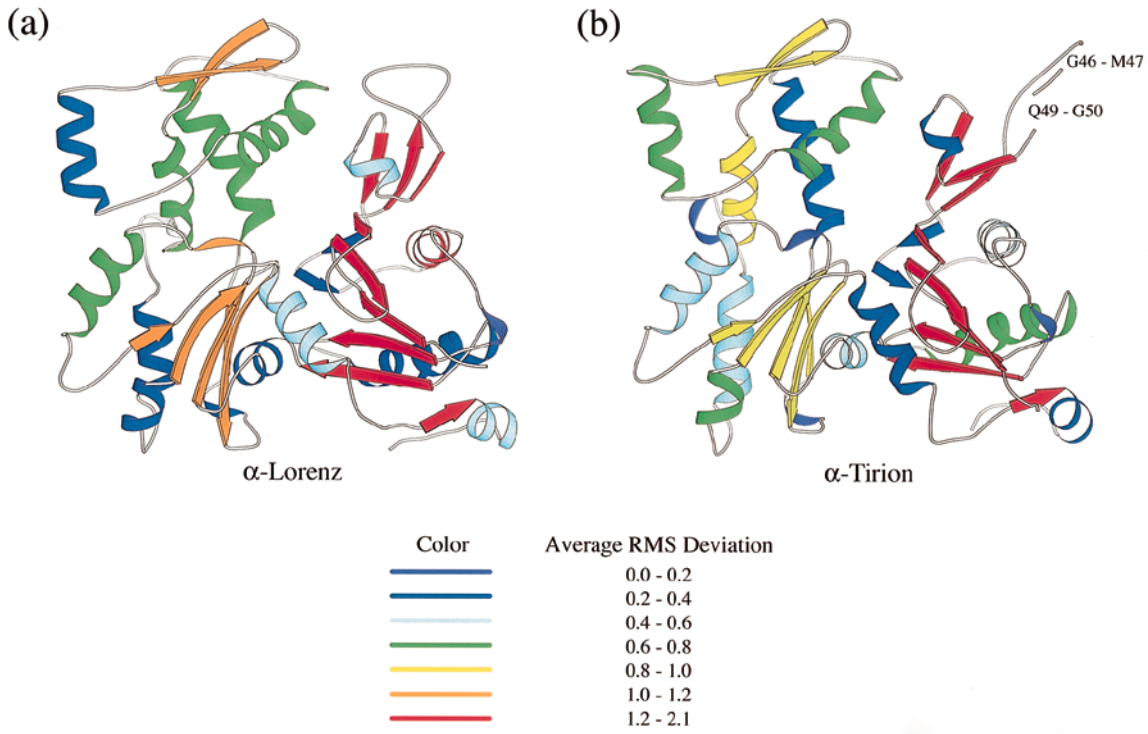

Figure 6. Changes in F-actin secondary structure are not consistent with the constraints on actin conformational change determined in this analysis. Each element of secondary structure in the F-actin model (α-Lorenz and α-Tirion) was superimposed onto the unbiased average conformations (see Figure 2) and the rms deviations between them calculated. The rms deviations between the secondary structural elements are mapped onto the models above using the listed color code. The secondary structural elements undergo significant changes compared to the differences observed between the four actin crystal structures shown in Figure 2. (Note, the distances between the α-carbon atoms of residues G46-M47 and Q49-G50 in the F-actin Tirion model are greater than the limit set by the MOLSCRIPT program, which is why they are not plotted.)

larity to hexokinase, glyceraldehyde-3-phosphate dehydrogenase (GAPDH) and alcohol dehydrogenase (ADH), proteins that have been observed crystallographically to change conformation upon ligand binding (Gerstein *et al.*, 1994). Each of these proteins has two major domains whose structural features can be characterized as *XBA:abx* layering (Gerstein *et al.*, 1994), with the cleft occurring between *A* and *a*. Layers *XBA* make up a rigid domain and layers *abx* make up a mobile domain. Specifically, each domain consists of an α-helix (*A/a*), followed by a β-sheet (*B/b*) and a third layer (*X/x*) made up of either β-strands, α-helices or both, depending on the protein. The ligand binding site is located between the rigid and mobile domains. The crossed α-helices (*A/a*) function to connect the domains and to form the base of the ligand binding site. Upon ligand binding, layers *a,b* and *x* of the mobile domains of hexokinase, GADPH and ADH have been described as sliding past one another, as they envelope the ligand (Gerstein *et al.*, 1994).

In the case of the actin structures compared here, the mechanism of conformational change is better described as a rotation of two rigid domains, facilitated by small conformational changes distributed throughout residues in the crossed helices, with an additional rotation of a semi-rigid domain. First, the results of this study show that layers *a* and *b* and two helices from layer *x* of the actin ''mobile'' domain actually form a rigid core, the small domain core, and do not slide past one another. In addition, most of the rotational change between the two domains of the β-actin open and tight states can be best simulated by small changes in the torsion angles of the backbone residues of helix *A*. However, consistent with the previously proposed sliding mechanism (Gerstein *et al.*, 1994), it is observed that subdomain 2, constituting the remainder of layer *x* in actin, does move independently of layers *a* and *b*.

It might be argued that the mechanism of domain closure in actin might differ from hexokinase, GADPH and ADH because the unliganded form of actin was not included in the analysis. However, upon further examination of these structures, we find that the other members of this family actually share a mechanism of conformational change more similar to that of actin. In GADPH and ADH, layers *a* and *b* and the helices of layer *x* do not slide past one another, but form a rigid core, analogous to actin (identified using the *sieve-fit* algorithm; data not shown). Like subdomain 2, an extended loop of GADPH, residues N31

to E70, forms an independent domain which rotates independently of this second rigid core. Thus, GADPH and ADH clearly change conformation *via* a similar mechanism to that of actin. Finally, in contrast to the other members of the family, layers *a*, *b* and *x* of hexokinase do not form a rigid core. In fact, the β-sheet (*b*) itself is not even rigidly maintained between both structures; the rms deviation of these sheets between the bound and unbound conformations is 0.9 Å. When the helices of layer *x* are included in this superposition, the rms deviation increases by only 0.1 Å. We predict that when higher resolution structures of hexokinase are determined, the sheet and helices of the ''mobile'' domain will form a rigid body, similar to what has been observed for actin, with the majority of the conformational change occurring only at the crossed helices.

Implications for alternative conformations of actin

We expect conformational changes in actin accompanying polymerization will occur mainly in the interdomain region and at the loops of subdomains 2 and 4, and that the structures of the rigid cores will be largely conserved, with the possible exception of residues S350 to Q354, which may influence the positioning of the C-terminal helix. This is at odds with what has been predicted for F-actin models on the basis of directed mutation algorithms or algorithms which used the actin normal modes as structural refinement parameters (Lorenz *et al*., 1993; Tirion *et al*., 1995). It is possible that actin represents an exception to the generalizations of Gerstein & Chothia (1991), and that large-scale changes in secondary structure take place throughout the molecule. However, we favor models in which the largest changes will occur in hinge and shear regions which separate rigid domains, regions where secondary and tertiary structure is largely maintained. Using the information obtained here, it is possible to generate alternative structures of the actin monomer which are consistent with the principles of conserved domains separated by flexible peptides and compatible with efficient packing into the helical actin filament.

Methods

The *sieve-fit* and *fit-all* algorithms were developed by Lesk (1991) and Gerstein & Chothia (1991), respectively. The algorithm for identifying an unbiased average structure was developed by Gerstein & Altman (1995). The programs based on these algorithms were coded by R. Page using subroutines to find the optimal superposition of three-dimensional protein structures provided by Sippl & Stegbuchner (1991). The outline of these algorithms and their use in identifying rigid domains and hinge and shear regions are described in Results. Figures 2, 4 and 6 were made using the graphics program MOLSCRIPT (Kraulis, 1991).

Acknowledgments

The authors thank Dr J. Chik and Dr M. Rozycki for valuable discussions, Dr M. Sippl for providing the superposition subroutines, Dr P. J. McLaughlin for making the α-actin:gelsolin-S1 structure coordinates available and Dr K. Holmes, Dr M. Lorenz and Dr M. Tirion for providing the coordinates of the F-actin models. This work was supported by grants from the National Institute of Health, GM-44038, the Swedish Natural Science Council and the Swedish Cancer Foundation. R. Page was supported by a predoctoral National Science Foundation Fellowship.

References

Allen, P. G., Laham, L. E., Way, M. & Janmey, P. A. (1996). Binding of phosphate, aluminum flouride or beryllium flouride to f-actin inhibits severing by gelsolin. *J. Biol. Chem.* **271**, 4665–4670.

Bennett, W. S. & Huber, R. (1984). Structural and functional aspects of domain motions in proteins. *CRC Crit. Rev. Biochem.* **15**, 291–384.

Bennett, W. S., Jr & Steitz, T. A. (1980). Structure of a complex between yeast hexokinase A and glucose. II. Detailed comparisons of conformation and active site configuration with the native hexokinase B monomer and dimer. *J. Mol. Biol.* **140**, 211–230.

Brunger, A. T., Huber, R. & Karplus, M. (1987). Trypsinogen-trypsin transition: a molecular dynamics study of induced conformational change in the activation domain. *Biochemistry*, **26**, 5153–5162.

Chik, J. K., Lindberg, U. & Schutt, C. E. (1996). The structure of an open state of β-actin at 2.65 Å resolution. *J. Mol. Biol.* **263**, 607–623.

Colonna-Cesari, F., Perahia, D., Karplus, M., Eklund, H., Braden, C. I. & Tapia, O. (1986). Interdomain motion in liver alcohol dehydrogenase. Structural and energetic analysis of the hinge bending mode. *J. Biol. Chem.* **261**, 15273–15280.

Flaherty, K. M., McKay, D. B., Kabsch, W. & Holmes, K. C. (1991). Similarity of the three-dimensional structures of actin and the ATPase fragment of a 70-kDa heat shock cognate protein. *Proc. Natl Acad. Sci. USA*, **88**, 5041–5045.

Frauenfelder, H. (1995). Proteins: paradigms of complex systems. *Experientia*, **51**, 200–203.

Frieden, C. & Parane, K. (1985). Differences in G-actin containing bound ATP or ADP: the Mg^{2+}-induced conformational change requires ATP. *Biochemistry*, **24**, 4192–4196.

Frieden, C., Lieberman, D. & Gilbert, H. (1980). A fluorescent probe for conformational changes in skeletal muscle G-actin. *J. Biol. Chem.* **255**, 8991–8993.

Gerstein, M. & Altman, R. (1995). Average core structures and variability measures for protein families: application to the immunoglobins. *J. Mol. Biol.* **251**, 161–175.

Gerstein, M. & Chothia, C. (1991). Analysis of protein loop closure. Two types of hinges produce one motion in lactate dehydrogenase. *J. Mol. Biol.* **220**, 133–149.

Gerstein, M., Schulz, G. & Chothia, C. (1993). Domain closure in adenylate kinase. Joints on either side of two helices close like neighboring fingers. *J. Mol. Biol.* **229**, 494–501.

Gerstein, M., Lesk, A. M. & Chothia, C. (1994). Structural mechanisms for domain movements in proteins. *Biochemistry,* **33**, 6739–6749.

Harrison, S. C., Olson, A. J., Schutt, C. E. & Winkler, F. K. (1978). Tomato bushy stunt at 2.9 Å resolution. *Nature,* **276**, 368–373.

Kabsch, W., Mannherz, H. G., Suck, D., Pai, E. F. & Holmes, K. C. (1990). Atomic structure of the α-actin:DNase I complex. *Nature,* **347**, 37–44.

Kim, E., Moroki, M., Seguro, K., Muhlrad, A. & Reisler, E. (1995). Conformational changes in subdomain 2 of F-actin: fluorescence probing by dansyl ethylenediamine attached to Gln-41. *Biophys. J.* **69**, 2024–2032.

Kraulis, P. J. (1991). MOLSCRIPT: a program to produce both detailed and schematic plots of protein structures. *J. Appl. Crystallog.* **24**, 946–950.

Lepault, J., Ranck, J., Erk, I. & Carlier, M. (1994). Small angle X-ray scattering and electron cryomicroscopy study of actin filaments: role of the bound nucleotide in the structure of F-Actin. *J. Struct. Biol.* **112**, 79–91.

Lesk, A. M. (1991). *Protein Architecture: A Practical Guide*, IRL Press, Oxford.

Lesk, A. M. & Chothia, C. (1984). Mechanisms of domain closure in proteins. *J. Mol. Biol.* **174**, 175–191.

Lorenz, M., Popp, D. & Holmes, K. C. (1993). Refinement of the F-actin model against X-ray fiber diffraction data by the use of a directed mutation algorithm. *J. Mol. Biol.* **234**, 826–836.

McLaughlin, P. J., Gooch, J. T., Mannherz, H. G. & Weeds, A. G. (1993). Structure of gelsolin segment 1α-actin complex and the mechanism of filament severing. *Nature,* **364**, 685–692.

Orlova, A. & Egelman, E. H. (1993). A conformational change in the actin subunit can change the flexibility of the actin filament. *J. Mol. Biol.* **232**, 334–341.

Orlova, A. & Egelman, E. H. (1995). Structural dynamics of F-actin: I. Changes in the C terminus. *J. Mol. Biol.* **245**, 582–597.

Orlova, A., Prochniewicz, E. & Egelman, E. H. (1995). Structural dynamics of F-actin: II. Cooperativity in structural transitions. *J. Mol. Biol.* **245**, 598–607.

Schutt, C. E., Myslik, J. C., Rozycki, M. D., Goonesekere, N. C. & Lindberg, U. (1993). The structure of crystalline profilin-β-actin. *Nature,* **365**, 810–816.

Schutt, C. E., Rozycki, M. D., Myslik, J. C. & Lindberg, U. (1995). A discourse on modeling F-actin. *J. Struct. Biol.* **115**, 186–198.

Sippl, M. J. & Stegbuchner, H. (1991). Superposition of three-dimensional objects: a fast and numerically stable algorithm for the calculation of the matrix of optimal rotation. *Comp. Chem.* **15**, 73–78.

Sprang, S. R., Acharya, K. R., Goldsmith, E. J., Stuart, D. I., Varvill, K., Fletterick, R. J., Madsen, N. B. & Johnson, L. N. (1988). Structural changes in glycogen phosphorylase induced by phosphorylation. *Nature,* **336**, 215–221.

Strezelecka-Golaszewska, H., Moraczewska, J., Khaitlina, S. Y. & Mossakowkska, M. (1993). Localization of the tightly bound divalent-cation-dependent and nucleotide dependent conformation changes in G-actin using limited protolytic digestion. *Eur. J. Biochem.* **211**, 731–742.

Strezelecka-Golaszewska, H., Wozniak, A., Hult, T. & Lindberg, U. (1996). Effects of the type of divalent cation, Ca^{2+} or Mg^{2+}, bound at the high-affinity site and of the ionic composition of the solution on the structure of F-actin. *Biochem. J.* **316**, 713–721.

Tirion, M. M., ben-Avraham, D., Lorenz, M. & Holmes, K. C. (1995). Normal modes as refinement parameters for the F-actin model. *Biophys. J.* **68**, 5–12.

Wriggers, W. & Schulten, K. (1997). Protein domain movements: detection of rigid domains and visualization of hinges in comparisons of atomic coordinates. *Proteins: Struct. Funct. Genet.* **29**, 1–14.

Zhang, X. J., Wozniak, J. A. & Matthews, B. W. (1995). Protein flexibility and adaptability seen in 25 crystal forms of T4 lysozyme. *J. Mol. Biol.* **250**, 527–552.

Edited by D. Rees

(Received 13 January 1998; received in revised form 20 April 1998; accepted 20 April 1998)